ACS OMEGA

Open Access

http://pubs.acs.org/journal/acsodf

Article

Unraveling Hydrogen Adsorption on Transition Metal-Doped $[Mo_3S_{13}]^{2-}$ Clusters: Insights from Density Functional Theory Calculations

Thu Thi Phung, Nguyen Thi Huyen, Nguyen Thi Giang, Nguyen Minh Thu, Nguyen Thanh Son, Nguyen Hoang Tung, Ngo Thi Lan, Son Tung Ngo, Nguyen Thi Mai, and Nguyen Thanh Tung*

Cite This: *ACS Omega* 2024, 9, 20467−20476

Read Online

ACCESS | Metrics & More | Article Recommendations | Supporting Information

ABSTRACT: Molecular and dissociative hydrogen adsorption of transition metal (TM)-doped $[Mo_3S_{13}]^{2-}$ atomic clusters were investigated using density functional theory calculations. The introduced TM dopants form stable bonds with S atoms, preserving the geometric structure. The S-TM-S bridging bond emerges as the most stable configuration. The preferred adsorption sites were found to be influenced by various factors, such as the relative electronegativity, coordination number, and charge of the TM atom. Notably, the presence of these TM atoms remarkably improved the hydrogen adsorption activity. The dissociation of a single hydrogen molecule on $TM[Mo_3S_{13}]^{2-}$ clusters (TM = Sc, Cr, Mn, Fe, Co, and Ni) is thermodynamically and kinetically favorable compared to their bare counterparts. The extent of favorability monotonically depends on the TM impurity, with a maximum activation barrier energy ranging from 0.62 to 1.58 eV, lower than that of the bare cluster (1.69 eV). Findings provide insights for experimental research on hydrogen adsorption using TM-doped molybdenum sulfide nanoclusters, with potential applications in the field of hydrogen energy.

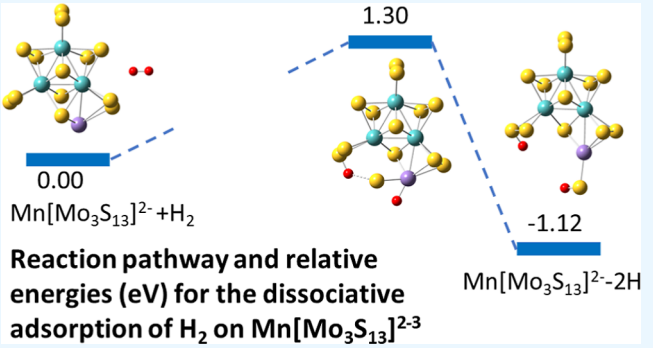

INTRODUCTION

To address one of the most pressing global challenges concerning future energy resources, researchers have explored the potential of hydrogen energy as an alternative to fossil fuels, given its clean emissions, abundance, and renewability. Consequently, numerous studies have focused on different hydrogen-producing methods,[1] and water splitting has emerged as a highly promising technique, offering significant advantages such as environmental friendliness, sustainability, and high product purity.[2] However, the main obstacle hindering its widespread industrial application lies in the sluggish kinetics of the hydrogen evolution reaction (HER) involved in the water-splitting process.[3,4] To overcome this challenge, catalysts have become pivotal factors, playing a crucial role in promoting efficient HER kinetics.

Despite the great efficiency of Pt and its derivatives in HER as well as the water-splitting process,[5,6] their scarcity and high cost necessitate the exploration of alternative materials that can meet performance requirements, cost-effectiveness, and reduced processing time. Among potential candidates, nanostructured molybdenum sulfide (MS) configurations have garnered attention due to their higher density of active sites compared to other materials.[7−10] Particularly, the amorphous structure constructed by $[Mo_3S_{13}]^{2-}$ clusters with its triangular framework consisting of three bridging, three-terminal, and one apical *S* has shown promising potential as the most active form in the HER catalysis among various MS configurations.[10−13] While considerable efforts have been made to enhance the MS catalytic activity by employing TM dopants as an intriguing strategy, the underlying interaction between hydrogen atoms and the MS catalyst with specific active sites has not yet been fully understood. For instance, experimental results combined with density functional theory (DFT) calculations indicated that HER is hindered by the bond between Co-dopant and MoS_2, but is improved when Co is replaced with Ni.[14] Meanwhile, Martinez and co-workers reported an opposite finding, where HER is increasing with Co doping over Ni one as $CoMoS_2 > MoS_2 > NiMoS_2$.[15]

As the catalytic process unfolds after molecular hydrogen adsorption, followed by hydrogen activation and dissociation or recombination, studying hydrogen adsorption and dissociation is fundamental to understanding the nature of catalysts.

Received: February 18, 2024
Revised: April 4, 2024
Accepted: April 10, 2024
Published: April 26, 2024

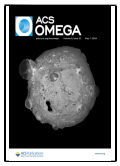

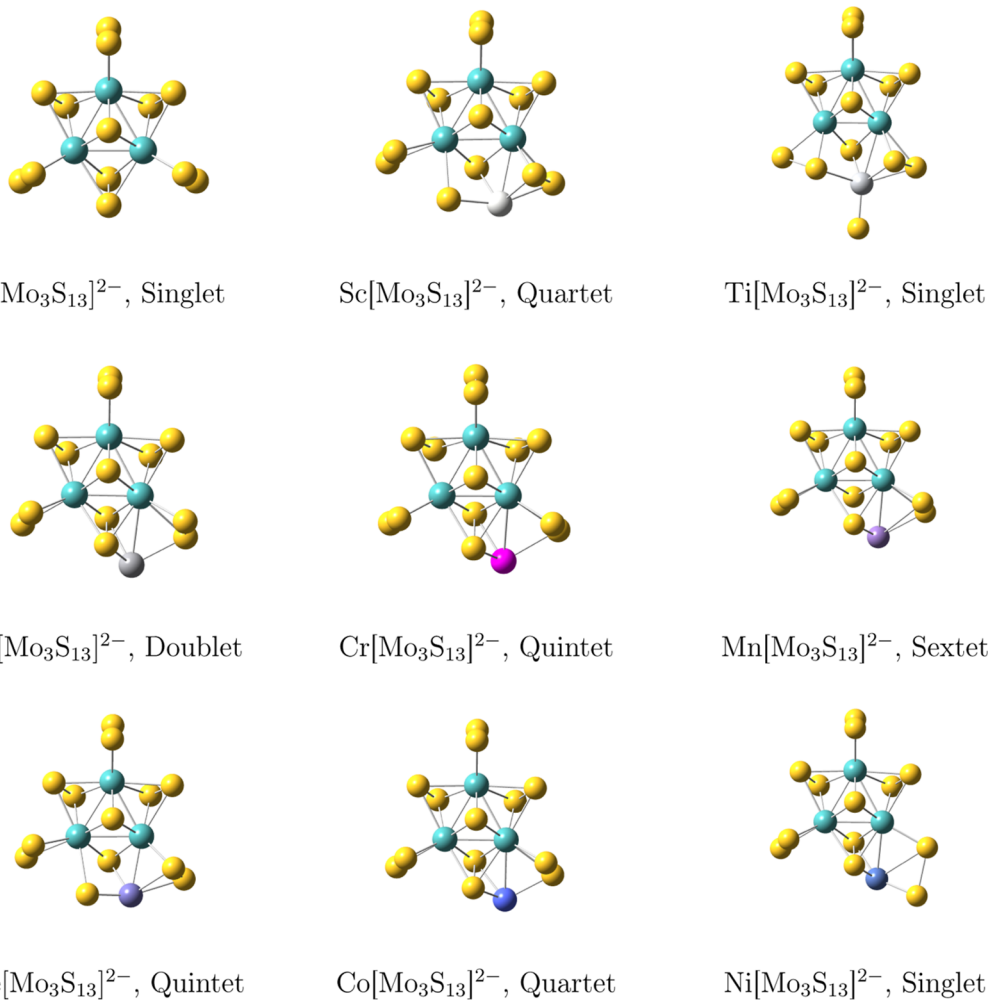

Figure 1. Lowest-energy configurations of bare $[Mo_3S_{13}]^{2-}$ and $TM[Mo_3S_{13}]^{2-}$ (TM = Sc, Ti, V, Cr, Mn, Fe, Co, and Ni) clusters. Turquoise, yellow, and red spheres denote Mo, S, and H, respectively. Light gray, gray, dark gray, pink, violet, slate blue, blue, and royal blue spheres represent Sc, Ti, V, Cr, Mn, Fe, Co, and Ni, respectively.

In this context, a more in-depth understanding at the molecular level regarding the interaction between hydrogen molecules and potential adsorption surfaces becomes essential. This is precisely where nanoclusters, composed of a few atoms, prove to be valuable as an effective model for catalytic systems. They offer profound insights into potentially reactive sites due to their ability to exhibit significant variations in physical and chemical properties with different sizes and compositions.[16−18] Among various methodologies, DFT calculations have demonstrated their effectiveness in evaluating the hydrogen adsorption capacity of doped metal clusters, making them promising catalysts for water splitting.[19,20] For example, research by Ma and co-workers demonstrated that Pd_xNi_y clusters exhibit superior adsorption activity compared to their pure counterparts.[20] In a similar vein, Lan et al. found that Au_9TM^{2+} clusters exhibit diverse hydrogen molecular absorption configurations, depending on the specific TM dopant.[21] Investigations into the impact of dopant atom size and coordination number on adsorption behavior have been conducted for Al_nCr and $Al_nRh_2^+$ clusters, as reported by Jia and co-workers.[22,23] Furthermore, Boruah et al. observed that the molecular hydrogen adsorption properties of Mg_3TM clusters are influenced not only by the type of transition metal (TM) dopant but also by its charge state.[24] Additionally, German et al. found that the presence of Nb and Zr in MgH_2 clusters can weaken the bond strength between Mg and H atoms.[25] Unfortunately, there appears to be a notable deficiency in the comprehension of $[Mo_3S_{13}]^{2-}$ clusters within this particular context, and consequently, further investigation into this area is highly warranted.

In this study, we investigated the hydrogen adsorption behavior of $[Mo_3S_{13}]^{2-}$ clusters doped with various TMs (TM = Sc−Ni). A thorough analysis of the lowest-energy structures, charge transfer, hydrogen adsorption energy, and energy profiles has been performed. Our DFT results demonstrated that the inclusion of typical TM dopants can significantly enhance the reactivity of hydrogen adsorption on the $[Mo_3S_{13}]^{2-}$ cluster.

MODELS AND METHODS

We utilized DFT calculations to optimize these structures and assess their interactions with hydrogen. Specifically, the B3LYP density functional method, a well-established and reliable approach, in conjunction with the LanL2DZ basis set embedded in the Gaussian 09 package was employed for all calculations.[26] The choice of the B3LYP functional was grounded by its proven accuracy in previous studies involving Mo−S clusters.[27,28] We further validate the reliability and

https://doi.org/10.1021/acsomega.4c01557
ACS Omega 2024, 9, 20467−20476

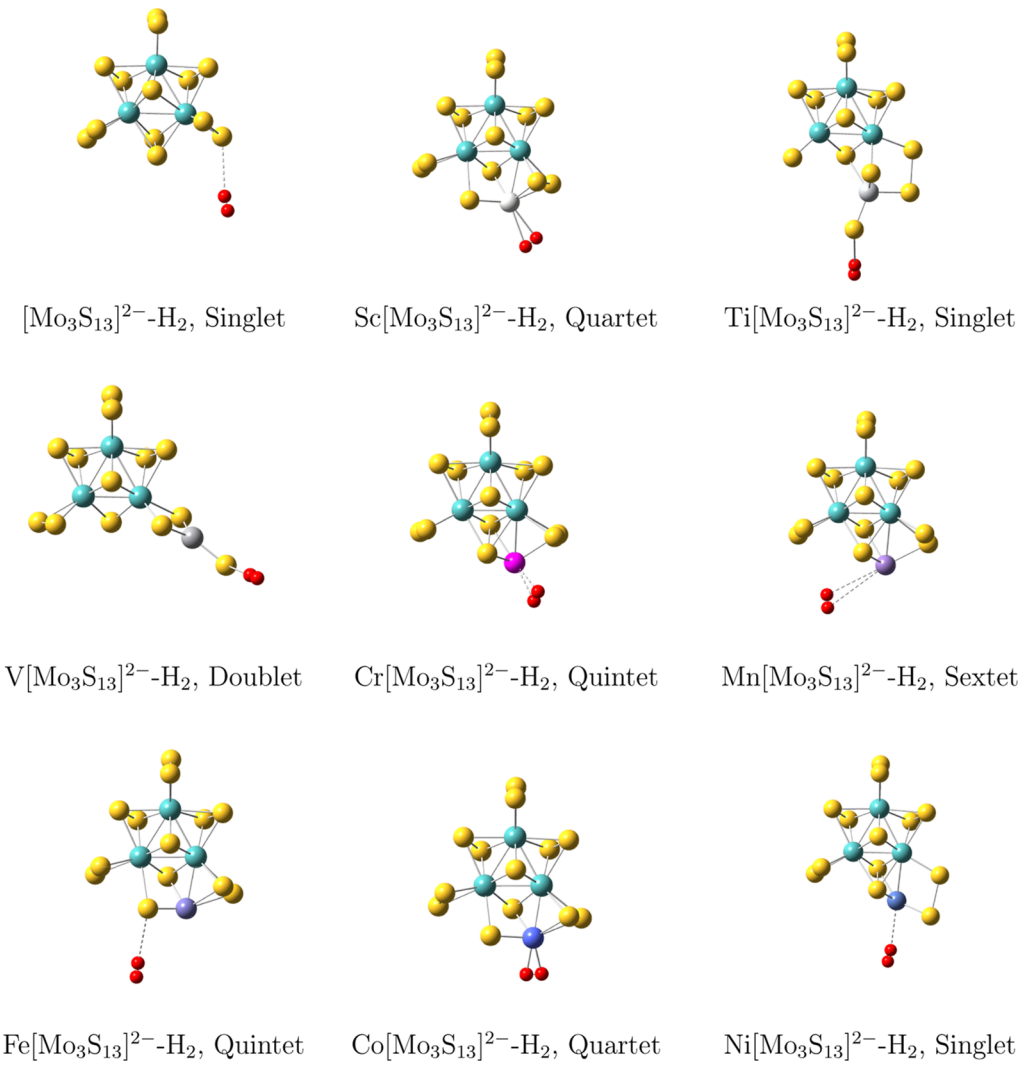

Figure 2. Lowest-energy configurations of bare $[Mo_3S_{13}]^{2-}$−H_2 and $TM[Mo_3S_{13}]^{2-}$−H_2 (TM = Sc, Ti, V, Cr, Mn, Fe, Co, and Ni) clusters. Turquoise, yellow, and red spheres denote Mo, S, and H, respectively. Light gray, gray, dark gray, pink, violet, slate blue, blue, and royal blue spheres represent Sc, Ti, V, Cr, Mn, Fe, Co, and Ni, respectively.

accuracy of our calculations by assessing the binding energy of TM-S dimers by using various functional combinations (B3LYP, B3P86, B3PW91, and PBEPBE) in conjunction with the LanL2DZ and SDD basis sets. The outcomes are compared with available experimental results and summarized in Table S1. The computed binding energies of TM-S with B3LYP/LanL2DZ are in the closest agreement with experimental values. For the optimization, two approaches were applied in parallel. First, a larger number of $TM[Mo_3S_{13}]^{2-}$ potential structures were generated using the stochastic algorithm.[29] Concurrently, various initial structures for TM-$[Mo_3S_{13}]^{2-}$ clusters were manually constructed by placing a TM atom at all feasible positions within the experimentally verified $[Mo_3S_{13}]^{2-}$ structure.[13] After the energy optimization, the most stable $TM[Mo_3S_{13}]^{2-}$ was utilized to build hydrogen absorbed configurations. Either a single hydrogen molecule or two hydrogen atoms are introduced at different sites within the optimized $TM[Mo_3S_{13}]^{2-}$ structures to explore the most stable configurations. To ensure structural stability and confirm the existence of these configurations as energy minima on the potential energy surface, their vibrational frequencies were calculated and examined. Moreover, all possible spin multiplicities were considered for each geometry to secure the reliability of the ground-state optimization process. To determine the transition state (TS) of the ground-state structures, the quadratic synchronous transit method was performed.[30] This involved conducting scans of the relaxed potential energy surface while appropriately varying the internal coordinates. For the convergence conditions in our calculations, we set the following threshold parameters: 2.0×10^{-5} Hartree for energy and 5.0×10^{-3} Ångströms for displacement.

RESULTS AND DISCUSSION

Optimized Geometric Structure. In our calculations, a series of geometrical and spin isomers were found to satisfy the convergence condition using the B3LYP/LanL2DZ approach. Nevertheless, only the lowest-energy isomers without imaginary frequencies are considered and analyzed for hydrogen adsorption activity. Figures 1−3 depict the optimized structures of $[Mo_3S_{13}]^{2-}$, $[Mo_3S_{13}]^{2-}$−H_2, $[Mo_3S_{13}]^{2-}$−2H, $TM[Mo_3S_{13}]^{2-}$, $TM[Mo_3S_{13}]^{2-}$−H_2, and $TM[Mo_3S_{13}]^{2-}$−2H clusters.

https://doi.org/10.1021/acsomega.4c01557
ACS Omega 2024, 9, 20467−20476

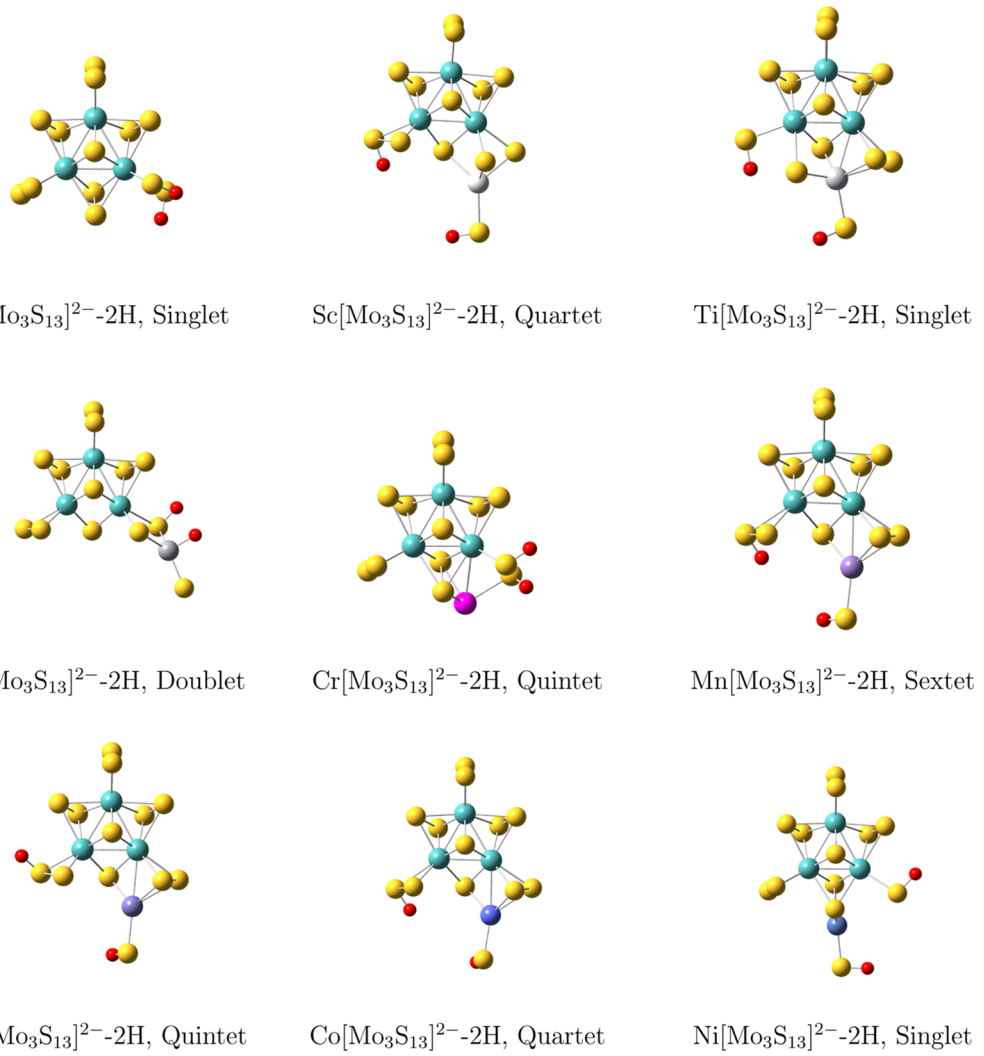

Figure 3. Lowest-energy configurations of bare $[Mo_3S_{13}]^{2-}$−2H and $TM[Mo_3S_{13}]^{2-}$−2H (TM = Sc, Ti, V, Cr, Mn, Fe, Co, and Ni) clusters. Turquoise, yellow, and red spheres denote Mo, S, and H, respectively. Light gray, gray, dark gray, pink, violet, slate blue, blue, and royal blue spheres represent Sc, Ti, V, Cr, Mn, Fe, Co, and Ni, respectively.

Upon initial examination, it is observed that the TM dopant prefers to reside between the terminal and bridging disulfides of the bare $[Mo_3S_{13}]^{2-}$ cluster, maximizing the coordination number and forming stable S-TM-S bridging bonds. Similar behavior was reported when TM is doped into the Au $^{2+}_{10}$ cluster.[31] While V, Cr, or Co doping induces a trivial distortion in the geometrical structure of $[Mo_3S_{13}]^{2-}$, the S−S bond length of bridging and terminate S^{2-} is considerably stretched when Sc, Ti, Mn, Fe, or Ni is introduced. The calculated dissociation energies of $TM[Mo_3S_{13}]^{2-}$ clusters through the loss of either a TM atom, an S atom, or a TM-S dimer (see Figure S1 in Supporting Information) suggest that the TM atom establishes a stronger bond with the cluster compared to an S atom or a TM-S dimer. Although the initial geometric framework of the bare cluster is largely preserved during the introduction of a TM atom, the S−S bond distance near the TM atom elongates in certain species following the adsorption of hydrogen molecules such as those doped with Ti, V, and Co. This suggests a notable interaction between hydrogen and both S and TM atoms within these species. However, no structural modifications are observed in the remaining configurations, $TM[Mo_3S_{13}]^{2-}$ (TM = Sc, Cr, Mn, Fe, and Ni) clusters, regarding the H_2−cluster interaction, suggesting their high structural stability toward the adsorption of a hydrogen molecule.

In bare clusters, the hydrogen molecule favors attaching at the S atoms belonging to terminal S^{2-} compared to other sites. The terminal-site preference is also observed in $TM[Mo_3S_{13}]^{2-}$−H_2 with TM = Sc, Cr, Mn, Co, and Ni. This phenomenon can be attributed to the electronegativity χ difference among TM (1.36−1.91) and H (2.20) compared to those of S (2.58) and Mo (2.16). Given that bonding fundamentally arises from electrostatic attraction facilitated by electron transfers between atoms with substantial electronegativity differences, the establishment of bonds between the surface TM and H_2 is therefore typically favorable.[23,31,32] Not only the electronegativity but also the atomic coordination number (N) have been demonstrated to be an important factor in elucidating the preferred adsorption site for hydrogen. For example, investigations involving Al_nRh^+ cationic clusters, employing time-of-flight mass spectrometric and infrared multiple photon dissociation spectroscopic methods, have revealed a propensity for hydrogen to bind to the Al atom for specific cluster sizes, particularly when the Rh impurity is either encapsulated or coordination-saturated.[23] In the realm of gold nanoparticles, adsorption energy calculations have unveiled an

https://doi.org/10.1021/acsomega.4c01557
ACS Omega 2024, 9, 20467−20476

inverse relationship between the coordination number of a surface atom and its adsorption energy, implying that an atom with lower coordination is more favorably suited for adsorption.[33] This principle helps understand the preference of hydrogen to attach to an unsaturated vertex S atom (N_S = 1 or 2) rather than a TM dopant (N_{Ti} = 4, N_V = 3, and N_{Fe} = 5) in instances like $Ti[Mo_3S_{13}]^{2-}-H_2$, $V[Mo_3S_{13}]^{2-}-H_2$, and $Fe[Mo_3S_{13}]^{2-}-H_2$ clusters, where competition between electronegativity and coordination occurs. Similarly, reports on hydrogen adsorption on Ag_nCr, Al_nCr, Au_9TM^{2+}, and $Al_nRh_2^+$ clusters emphasize the predominant influence of the low coordination of the impurity atom in determining the adsorption site selection.[21,22,34,35] Taking into account the phase space effect on product distributions could enhance the depth of our discussion. In this regard, we have included the calculation results of the entropy gradient ΔS for hydrogen atomic and molecular absorption reactions in Table S2. Notably, it is evident that the ΔS for the dissociative adsorption reaction is greater than that for the molecular adsorption one. This observation is consistent with the earlier discussion. Specifically, H_2 molecules tend to approach the surface of $TM[Mo_3S_{13}]^{2-}$ clusters, undergo molecular adsorption, and subsequently dissociate to form strong bonds with atomic clusters (excluding V-doped species).

Following molecular adsorption, the potential for the adsorbed hydrogen molecule to dissociate exists, which could lead to structural transformations within the clusters.[22,23,34] However, our calculations reveal that for the studied clusters, the ground-state structure is generally preserved, as illustrated in Figure 3. Most structures exhibit slight distortions, with either the dopant atom or S atom moderately displaced compared to their molecule-adsorbed counterparts. In contrast to molecule-adsorbed configurations, H atoms tend to prefer interaction with S atoms rather than TM atoms in $TM[Mo_3S_{13}]^{2-}-2H$. Interestingly, in both molecular and dissociative absorption configurations, the S−H bonds predominantly occur on terminal S, aligning with previous studies highlighting the stability of hydrogen-containing structures on the surface of MoS_2.[36−38] A divergence is observed in the V-doped species, where hydrogen atoms preferentially adsorb on both S and TM atoms. This results in an energy profile for $V[Mo_3S_{13}]^{2-}$ that differs from those of other structures, a topic that will be further discussed later.

Hydrogen Adsorption Analysis. Adsorption is commonly defined as the process of accumulating small molecules on a surface. Hydrogen adsorption is generally classified into molecular adsorption, characterized by weak van der Waals forces, and dissociative adsorption, involving chemical bonding, based on how molecules accumulate. Dissociative adsorption often occurs, although not necessarily, after molecular adsorption. Various factors, including the specific host species, type of adsorption, and energy barriers between molecules, atoms, and surfaces, can influence this process. Exploring the adhesion of a single hydrogen molecule to a precisely defined nanocluster becomes intriguing as a model for gaining fundamental insights into adsorption.[21−23,34,35]

To understand the binding nature of adsorbed hydrogen molecules on bare $[Mo_3S_{13}]^{2-}$ and doped $TM[Mo_3S_{13}]^{2-}$ clusters, the densities of electronic states (DOS) of both molecular and dissociative adsorption configurations are computed and plotted in Figures S2−S5. Corresponding partial and total DOSs are presented in each graph, where the solid and dashed lines indicate the states with spin-up (α) and spin-down (β) orientations, respectively. In $[Mo_3S_{13}]^{2-}-H_2$ and $TM[Mo_3S_{13}]^{2-}-H_2$ clusters, the majority of electronic states associated with the adsorbed hydrogen are located at the lower-energy side (less than −7.0 eV), clearly separated from the cluster states that extend beyond −6 eV. Considering the absence of overlap between hydrogen and cluster states, it can be affirmed that for both bare and doped clusters, the signal of chemical bonding between hydrogen and these species is relatively minor, potentially negligible. This observation is in line with previous studies on molecular adsorption of TM-doped silver or gold clusters, where van der Waals forces and/or electrostatic interaction between charge-polarized hydrogen and clusters can be potential bonding mechanisms.[22,23] Significantly, the peak linked to H_2 adsorption on Sc-, Cr-, and Co-doped species occurring below −9.0 eV exhibits a remarkable separation from the cluster states (positioned above −5.5 eV), indicating a notably weak binding between them compared to other doped and bare clusters.

The DOS for dissociative configurations in both bare $[Mo_3S_{13}]^{2-}-2H$ and doped $TM[Mo_3S_{13}]^{2-}-2H$ clusters exhibits a distinctive profile compared to that of their molecular adsorption counterparts. Notably, for both bare and doped species, the electronic states of hydrogen diffuse significantly toward higher energies, generally exceeding −6.0 eV, except for Mn- and Co-doped ones, indicating substantial hybridization with the cluster states as well as the formation of chemical bonding between hydrogen atoms and clusters. Simultaneously, the distinct pure attribute of H_2 at lower energies is no longer observable, as anticipated. For $Mn[Mo_3S_{13}]^{2-}-2H$ and $Co[Mo_3S_{13}]^{2-}-2H$ clusters, the electronic states of hydrogen are situated on the lower-energy side (approximately −7.0 eV), separated from the cluster states but overlapping with those of 3s-S orbitals. It is also noteworthy that the highest occupied molecular orbital states predominantly arise from the influence of 3s-S orbitals. As bonding processes typically entail electron transfers, this observation provides backing for the previous argument that surface S sites are preferred in the dissociative adsorption of hydrogen.

To gain insight into the adsorption mechanism of H_2 onto $TM[Mo_3S_{13}]^{2-}$ clusters, we calculated adsorption energy (E_{ads}) and H−H bond length for all structures of molecular adsorption and dissociative adsorption. E_{ads} can be defined by the following equations

$$E_{ads}(TM[Mo_3S_{13}]^{2-} - H_2) = E(TM[Mo_3S_{13}]^{2-}) + E(H_2) - E(TM[Mo_3S_{13}]^{2-} - H_2) \quad (1)$$

$$E_{ads}(TM[Mo_3S_{13}]^{2-} - 2H) = E(TM[Mo_3S_{13}]^{2-}) + E(H_2) - E(TM[Mo_3S_{13}]^{2-} - 2H) \quad (2)$$

The adsorption energy is quantified as the discrepancy between the cumulative energy of reactants and products, as depicted by eqs 1 and 2. This measure also signifies the minimal energy required to liberate the adsorbates from the surface. As indicated in Table 1, the calculated E_{ads} values for clusters are predominantly positive, except for $Cr[Mo_3S_{13}]^{2-}-H_2$ and $Co[Mo_3S_{13}]^{2-}-H_2$, suggesting that the hydrogen adsorption is generally favorable for the majority of the studied species. For molecular adsorption, the clusters exhibit a

https://doi.org/10.1021/acsomega.4c01557
ACS Omega 2024, 9, 20467−20476

Table 1. Calculated Adsorption Energies (ZPE Corrections Are Included) $E_{ads}(H_2)$ (in eV) and the H−H Bond Lengths d(H−H) (in Å) for Hydrogen Molecular and Dissociate Adsorption on TM$[Mo_3S_{13}]^{2-}$ (TM = Sc−Ni) Clusters

	E_{ads}		d(H−H)		d(H$_2$−S/TM)	d(H−S)
	−H$_2$	−2H	−H$_2$	−2H	−H$_2$	−2H
bare	−1.41	0.40	0.75	2.65		1.38
Sc	0.04	2.22	0.76	4.97	2.46	1.38
Ti	0.55	0.93	0.75	4.61	3.48	1.38
V	2.02	1.55	0.75	2.72	3.51	1.38/1.62
Cr	−0.01	0.51	0.76	2.70	2.26	1.38
Mn	0.01	1.12	0.75	4.07	3.64	1.38
Fe	0.01	1.53	0.75	6.72	3.56	1.38
Co	−0.20	0.92	0.76	4.39	2.06	1.38
Ni	0.01	0.94	0.75	6.03	3.32	1.38

relatively broad range of E_{ads} from −0.20 to 2.02 eV, while that for dissociative adsorption spans from 0.51 to 2.22 eV. Although the bare $[Mo_3S_{13}]^{2-}$ cluster is likely to adsorb hydrogen in dissociative form (E_{ads} = 0.40 eV), it requires at least an energy of 1.41 eV for hydrogen to attach the cluster in molecular form. Lower H_2 adsorption energy for smaller Mo_xS_y (x = 2 and y = 2−6; x = 4 and y = 4−6) clusters from 0.12−0.49 eV was reported by Chen and co-workers.[39] The dissociation of a hydrogen molecule on the Mo_3S_3 cluster takes place preferentially, while the molecular hydrogen absorption is implemented more easily on the Mo_2S_4 cluster. Nevertheless, that work indicated that the hydrogen atoms primarily absorb on Mo sites rather than S sites.[39] Baloglou and colleagues reported that hydrogen atoms preferentially form S−H bonds over S−Mo bonds in the $[Mo_3S_{13}]^{2-}$ cluster and its protonated forms,[40] being consistent with our result. Meanwhile, doping with TM remarkably changes the hydrogen adsorption feature of $[Mo_3S_{13}]^{2-}$. The dissociative-adsorption energy for TM$[Mo_3S_{13}]^{2-}$ clusters (from 0.51 to 2.22 eV) increases compared to that of bare $[Mo_3S_{13}]^{2-}$ (0.40 eV), implying that TM doping improves the dissociation preference of adsorbed H_2. In particular, the E_{ads} values of all TM$[Mo_3S_{13}]^{2-}$−2H clusters, with the exception of TM = V, are considerably higher than those of their corresponding molecular-adsorption species, indicating that the dissociation of the adsorbed hydrogen molecule is an exothermic process and thermodynamically preferred. It is noteworthy that the molecular adsorption energy of Sc, Cr, Mn, Fe, Co, or Ni-doped clusters is nearly zero or even negative, which indicates their neutrality to the adsorption or release of the H_2 molecule. This suggests an intriguing but competitive scenario wherein, upon approaching the surface of these clusters, the hydrogen molecule can rapidly detach from the clusters or simultaneously undergo dissociation, ultimately forming strong atomic bonds with the host cluster. The detachment of the adsorbed hydrogen molecule can even dominate in the latter case since several intermediate and TSs need to be overcome during the molecular dissociation process before reaching the final dissociative configuration. This is in line with the theoretical prediction that the ideal adsorption energy of a hydrogen molecule in solid materials should be from 0.2 to 0.6 eV.[41] With this picture in mind, one may agree that Ti$[Mo_3S_{13}]^{2-}$ has more potential to achieve molecular adsorption (E_{ads} = 0.55 eV), followed by a dissociative one (E_{ads} = 0.93 eV). In the opposite way, V$[Mo_3S_{13}]^{2-}$ does not comply with this behavior. Its molecular adsorption E_{ads} (2.02 eV) is considerably larger than the dissociative one (1.55 eV), suggesting that the dissociation of the adsorbed hydrogen molecule is energetically less preferred. Note that the interaction of the clusters and H_2 does not change the H−H bond length, being about 0.75−0.76 Å, compared to that of isolated hydrogen molecules (approximately 0.75 Å).[42] The bond length between TM$[Mo_3S_{13}]^{2-}$ and H_2 confirms the physisorption mechanism of the hydrogen molecule on the clusters. Meanwhile, there is a variation of the H_2−S/H_2-TM distance from 2.06 to 3.64 Å. In the chemisorption configuration, the adsorbed hydrogen molecule proceeded to evolve on the cluster surface, with the H−H distance considerably increasing in the window of 2.7−6.03 Å, suggesting a complete dissociation. This is well agreed with the results presented in Table 1, where a weaker bond between

Table 2. Calculated NBO Charge Distribution on TM$[Mo_3S_{13}]^{2-}$−2H and V$[Mo_3S_{13}]^{2-}$−H_2. Mo-1, Mo-2, and Mo-3 Represent Three Mo Atoms, while S-a and S-b Label Two S Atoms That Bind to the Corresponding H Atoms, H-a and H-b[a]

cluster	q(Mo-1)	q(Mo-2)	q(Mo-3)	q(S-a)	q(S-b)	q(TM)	q(H-a)	q(H-b)
Sc[Mo3S13]$^{2-}$−2H	−0.92	−1.33	−1.07	−0.53	−0.21	0.35	0.14	0.12
Sc$[Mo_3S_{13}]^{2-}$	−1.02	−1.30	−1.02	−0.29	−0.05	0.35		
Ti$[Mo_3S_{13}]^{2-}$−2H	−1.02	−1.29	−0.90	−0.28	−0.18	−0.59	0.13	0.14
Ti$[Mo_3S_{13}]^{2-}$	−0.89	−1.26	−0.94	−0.06	−0.09	−0.65		
V$[Mo_3S_{13}]^{2-}$−H_2	−1.04	−1.35	−1.09	−0.22		−0.26	0.04	−0.05
V$[Mo_3S_{13}]^{2-}$	−1.25	−1.29	−1.21	0.050		0.41		
Cr$[Mo_3S_{13}]^{2-}$−2H	−1.18	−1.29	−1.23	−0.25	−0.35	0.50	0.10	0.15
Cr$[Mo_3S_{13}]^{2-}$	−1.28	−1.30	−1.22	−0.02	−0.22	0.51		
Mn$[Mo_3S_{13}]^{2-}$−2H	−1.07	−1.31	−0.96	−0.65	−0.02	0.67	0.12	0.16
Mn$[Mo_3S_{13}]^{2-}$	−1.29	−1.30	−1.21	−0.05	−0.11	0.70		
Fe$[Mo_3S_{13}]^{2-}$−2H	−1.12	−1.31	−1.13	−0.21	−0.61	0.53	0.11	0.13
Fe$[Mo_3S_{13}]^{2-}$	−1.12	−1.30	−1.23	−0.09	−0.21	0.39		
Co$[Mo_3S_{13}]^{2-}$−2H	−1.11	−1.32	−0.96	−0.03	−0.60	0.39	0.16	0.11
Co$[Mo_3S_{13}]^{2-}$	−1.29	−1.30	−1.21	−0.11	−0.02	0.53		
Ni$[Mo_3S_{13}]^{2-}$−2H	−0.92	−1.29	−1.26	−0.14	−0.54	0.20	0.12	0.12
Ni$[Mo_3S_{13}]^{2-}$	−1.04	−1.29	−1.26	0.05	−0.31	0.09		

[a]In the case of molecular adsorption V$[Mo_3S_{13}]^{2-}$−H_2, both H-a and H-b bind to S-a atom. The corresponding q_{NBO} values without hydrogen adsorption are provided for comparison.

https://doi.org/10.1021/acsomega.4c01557
ACS Omega 2024, 9, 20467−20476

H_2 and the clusters is displayed by a variation from 2.06 to 3.64 Å for H_2−S/TM bond length, while after dissociating the H−S distance about 1.38 Å is independent of the cluster configurations.

Table 2 presents the calculated natural bond orbital (NBO) charge distribution on the most stable hydrogen-adsorbed TM$[Mo_3S_{13}]^{2-}$ clusters. The charge distribution undergoes a significant transformation at the S sites next to the TM atom compared to those without TM doping (see Table S3), underscoring the crucial role of the TM site in the interaction between the cluster and hydrogen species. Particularly, the TM atom donates electrons to neighboring S atoms, contributing to an increased electron density in the region between the bonds of the S-a and S-b atoms to the hydrogen atoms. This facilitates the formation of covalent bonds between the hydrogen and sulfur atoms. On the other hand, the charge on sulfur atoms adsorbing hydrogen generally becomes more negative compared to sulfur atoms without hydrogen adsorption, indicating a charge transfer between the cluster and hydrogen.[22] On another note, the negatively charged Mo atoms have saturated coordination numbers, making it challenging for these atoms to bind with hydrogen species. Consequently, the Mo atoms do not adsorb H atoms.

Next, we computed TS to gain a deeper understanding of the hydrogen dissociation pathway on the studied clusters. Figures 4−6 illustrate the dissociation pathway of bare and doped clusters with TM = Sc, Ti, Mn, Cr, and Fe, involving distinct TSs, each associated with a specific activation energy barrier and intermediates (I). The dissociation pathway of Co- and Ni-doped species is presented in the Supporting Information (Figures S6, S7). In addition, the corresponding intrinsic reaction coordinates for H_2 dissociation are shown in Figures S8−S14. In the bare $[Mo_3S_{13}]^{2-}$ cluster, the hydrogen molecule initially forms a bond with a terminal sulfur atom with an energy of 1.41 eV relative to that of the reactants. To reach the final dissociation state $[Mo_3S_{13}]^{2-}$−2H, positioned at an energy of −0.40 eV, an additional 0.28 eV is required to overcome a TS. This TS involves activation of the H_2 molecule, forming a more robust bond with the S atom.

While the hydrogen adsorption reaction on the bare $[Mo_3S_{13}]^{2-}$ cluster is relatively challenging, necessitating a high energy of 1.69 eV, this reaction occurs more readily in the TM$[Mo_3S_{13}]^{2-}$ clusters due to their considerably higher adsorption energies. In other words, TM$[Mo_3S_{13}]^{2-}$−2H clusters are thermodynamically stable with lower energies than reactants and corresponding TM$[Mo_3S_{13}]^{2-}$−H_2 clusters, typically −2.22 eV for TM = Sc, −0.93 eV for TM = Ti, −0.51 eV for TM = Cr, −1.12 eV for TM = Mn, −1.53 eV for TM = Fe, −0.92 eV for TM = Co, and −0.94 eV for TM = Ni. Importantly, the doping of TMs can serve as a potential strategy to alter the kinetics of the dissociative adsorption reaction. The maximum energy barriers vary depending on the dopant: 0.62 eV (Sc), 2.12 eV (Ti), 1.58 eV (Cr), 1.30 eV (Mn), 1.31 eV (Fe), 1.18 eV (Co), and 1.10 eV (Ni). Except for the Ti-doped cluster, where the barrier (2.12 eV) exceeds that on the bare cluster (1.69 eV), introducing the dopant generally lowers the activation barrier, suggesting enhanced reactivity. These results unveil that the hydrogen adsorption process on the TM$[Mo_3S_{13}]^{2-}$ cluster is not only thermodynamically favorable but also kinetically more favorable than that of the bare cluster with dopant-dependent dissociative pathways.

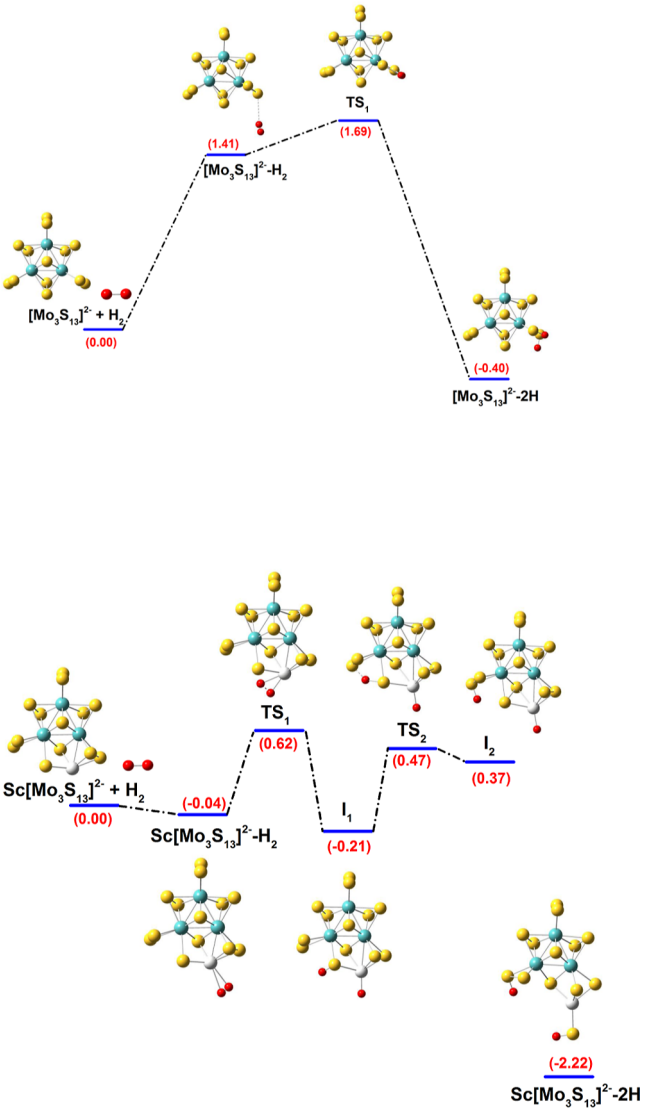

Figure 4. Calculated reaction pathways and relative energies (eV) for the molecular and dissociative adsorption of H_2 on bare- (singlet) and Sc-doped (quartet) clusters. Intermediates and TS_s are denoted as I_i and TS_i.

In more detail, the hydrogen adsorption and dissociative pathways of doped clusters occur in a more intricate manner than in a bare one. It can be seen that the kinetics of hydrogen dissociation in the TM$[Mo_3S_{13}]^{2-}$−H_2 cluster with TM = Sc, Mn, Co, Ni, and Fe are relatively similar. In this context, the adsorbed hydrogen molecule on the TM site gets activated and undergoes a separation to form bonds with S and TM atoms as it surmounts the activation barrier associated with a certain TS. The hydrogen atoms then diffuse further to bind with two S atoms in the resulting most stable structure. For example, to initiate the dissociation of the adsorbed hydrogen molecule on the Mn$[Mo_3S_{13}]^{2-}$ cluster, the TS_1 located at 0.89 eV, presents an active energy barrier of 0.90 eV compared with the H_2-adsorbed state (−0.01 eV). The adsorbed H_2 then undergoes separation into two hydrogen atoms, attaching to neighboring Mn and S sites (I_1). Subsequently, further hydrogen dissociation from I_1 to I_2 intermediates occurs after overcoming the second barrier TS_2 with an activation energy of 0.36 eV. Ultimately, the hydrogen dissociation process reaches a complete state where hydrogen atoms are bound to two

https://doi.org/10.1021/acsomega.4c01557
ACS Omega 2024, 9, 20467−20476

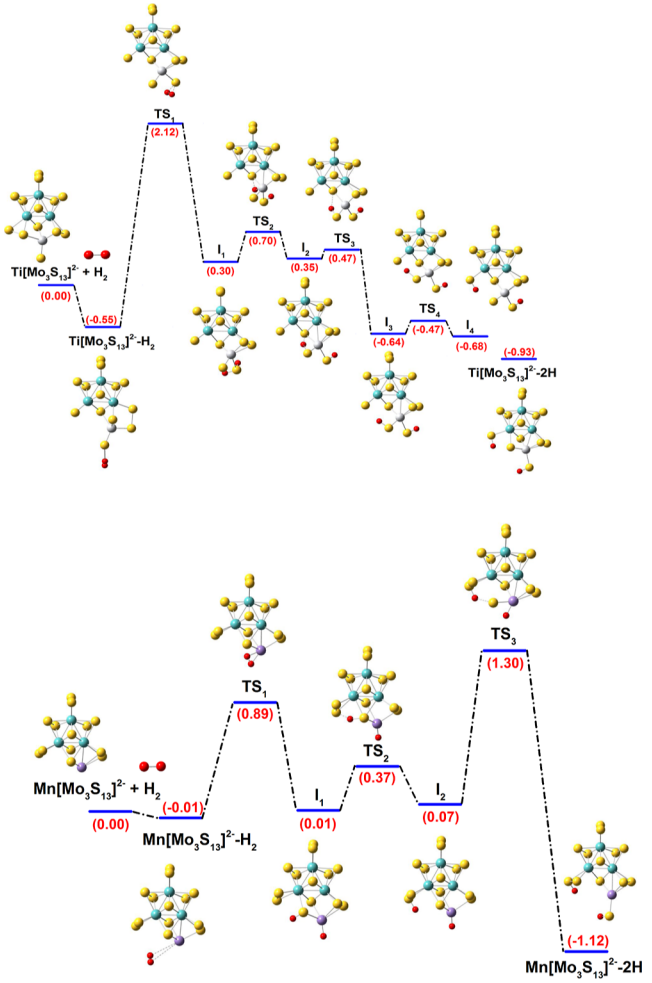

Figure 5. Calculated reaction pathways and relative energies (eV) for the molecular and dissociative adsorption of H_2 on Ti- (singlet) and Mn-doped (sextet) clusters. Intermediates and TSs are denoted as I_i and TS_i.

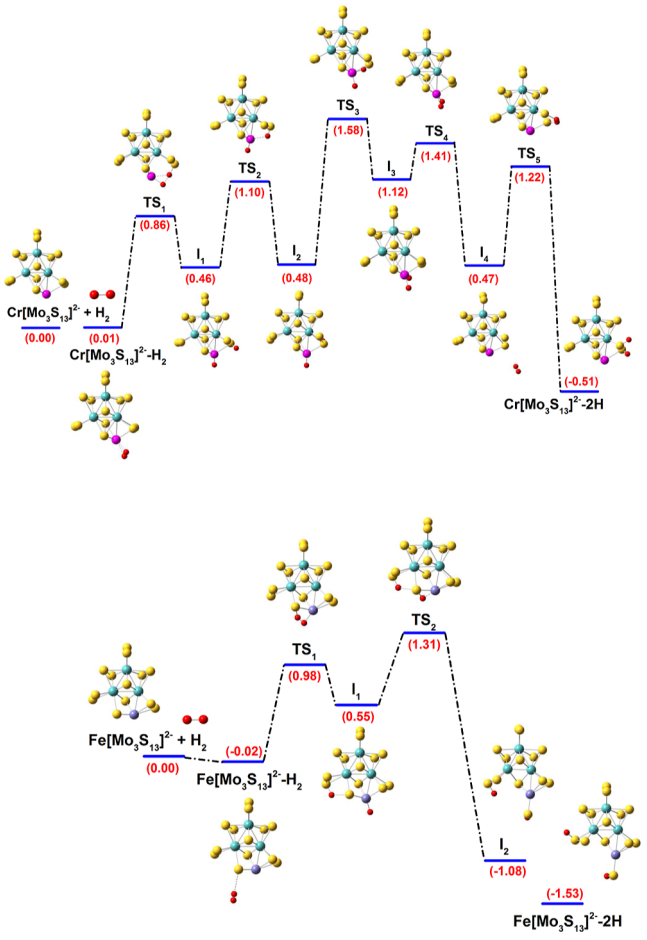

Figure 6. Calculated reaction pathways and relative energies (eV) for the molecular and dissociative adsorption of H_2 on Cr- (quintet) and Fe-doped (quintet) cluster. Intermediates and TSs are denoted as I_i and TS_i.

different S atoms, specifically terminal S^{2-} and bridging S^{2-}, upon overcoming the highest-energy TS_3 at 1.30 eV. In contrast to these species, the adsorbed hydrogen molecule in $Ti[Mo_3S_{13}]^{2-}$ prefers to establish bonds with sulfur atoms situated around the titanium atom during the dissociation process. Our calculations reveal that the reaction pathway of H_2 and $Cr[Mo_3S_{13}]^{2-}$ is notably complicated. The $Cr[Mo_3S_{13}]^{2-}$–H_2 cluster encounters five TS ranging from 0.86 to 1.58 eV, as shown in Figure 6, before attaining the final dissociative state at −0.51 eV. It is worth mentioning that the hydrogen dissociation on $Cr[Mo_3S_{13}]^{2-}$ reaches a temporary completion at the intermediate state I_2. However, two hydrogen atoms once again approach each other closely at I_3, and after overcoming the energy barrier at TS_4 (0.29 eV), they reunite to form a hydrogen gas molecule at I_4. In the final state, two hydrogen atoms are slightly separated and positioned on two neighboring sulfur atoms with a distance of 2.70 Å, resembling the configuration of the bare $[Mo_3S_{13}]^{2-}$ cluster (2.65 Å). This intriguing result highlights the potential of $Cr[Mo_3S_{13}]^{2-}$ clusters for hydrogen production applications.

CONCLUSIONS

The effect of TM atoms (TM = Sc–Ni) on the hydrogen adsorption reactivity of $[Mo_3S_{13}]^{2-}$ clusters is calculated within the DFT. The introduced TM dopants form stable bonds with S atoms at distinct sites without altering the overall geometric structure of the bare cluster. Notably, the S–TM–S bridging bond emerges as the most stable configuration, characterized by the lowest energy structure. TM atoms play a pivotal role in influencing hydrogen adsorption reactivity. The presence of TM atoms significantly enhances the kinetics of hydrogen adsorption on the surface of $TM[Mo_3S_{13}]^{2-}$ clusters. Except for $V[Mo_3S_{13}]^{2-}$ and $Ti[Mo_3S_{13}]^{2-}$, H_2 adsorption on $TM[Mo_3S_{13}]^{2-}$ clusters (TM = Sc, Cr, Mn, Fe, Co, and Ni) is found to be kinetically more favorable compared with the bare cluster, featuring maximum activation barrier energies ranging from 0.62 to 1.58 eV. This effect is attributed to the modification of the charge on neighboring S atoms, rendering them more negative compared to those in the bare cluster. Consequently, this alteration facilitates the formation of covalent bonds between hydrogen atoms and S atoms, resulting in the stabilization of the $TM[Mo_3S_{13}]^{2-}$–2H species. Our findings provide a robust understanding of experimental research on hydrogen adsorption using TM-doped MS nanoclusters. Moreover, these findings guide potential applications in hydrogen evolution water splitting reactions, highlighting the promising role of such clusters in advancing sustainable energy technologies.

https://doi.org/10.1021/acsomega.4c01557
ACS Omega 2024, 9, 20467−20476

■ ASSOCIATED CONTENT

Supporting Information

The Supporting Information is available free of charge at https://pubs.acs.org/doi/10.1021/acsomega.4c01557.

Comparison between calculated binding energies of TM-S dimer using different functionals and available experimental values; change in the conformational entropy in the adsorption reactions of a hydrogen atom or molecule on $TM[Mo_3S_{13}]^{2-}$ clusters; calculated NBO charge distribution in $[Mo_3S_{13}]^{2-}$ clusters; Cartesian coordinates of optimized $TM[Mo_3S_{13}]^{2-}$, $TM[Mo_3S_{13}]^{2-}$–H_2, and $TM[Mo_3S_{13}]^{2-}$–2H clusters; dissociation energies of $TM[Mo_3S_{13}]^{2-}$ according to different fragment pathways; DOS of lowest-energy molecular-adsorption configurations for $[Mo_3S_{13}]^{2-}$–H_2, $[Mo_3S_{13}]^{2-}$–2H, $TM[Mo_3S_{13}]^{2-}$–H_2, and TM-$[Mo_3S_{13}]^{2-}$–2H clusters; calculated energy profile for single H_2 adsorption and dissociation on $TM[Mo_3S_{13}]^{2-}$ clusters; and calculated intrinsic reaction coordinate for H_2 dissociation on $TM[Mo_3S_{13}]^{2-}$ clusters (PDF)

■ AUTHOR INFORMATION

Corresponding Author

Nguyen Thanh Tung − *Institute of Materials Science and Graduate University of Science and Technology, Vietnam Academy of Science and Technology, Hanoi 11307, Vietnam;* orcid.org/0000-0003-0232-7261; Email: tungnt@ims.vast.ac.vn

Authors

Thu Thi Phung − *Institute of Materials Science, Vietnam Academy of Science and Technology, Hanoi 11307, Vietnam; University of Science and Technology of Hanoi, Vietnam Academy of Science and Technology, Hanoi 11307, Vietnam*

Nguyen Thi Huyen − *Institute of Materials Science, Vietnam Academy of Science and Technology, Hanoi 11307, Vietnam*

Nguyen Thi Giang − *Institute of Materials Science, Vietnam Academy of Science and Technology, Hanoi 11307, Vietnam*

Nguyen Minh Thu − *Institute of Materials Science, Vietnam Academy of Science and Technology, Hanoi 11307, Vietnam*

Nguyen Thanh Son − *Institute of Materials Science, Vietnam Academy of Science and Technology, Hanoi 11307, Vietnam*

Nguyen Hoang Tung − *Institute of Materials Science, Vietnam Academy of Science and Technology, Hanoi 11307, Vietnam*

Ngo Thi Lan − *Institute of Materials Science, Vietnam Academy of Science and Technology, Hanoi 11307, Vietnam; Institute of Science and Technology, TNU-University of Sciences, Thai Nguyen City 250000, Vietnam*

Son Tung Ngo − *Laboratory of Biophysics, Institute for Advanced Study in Technology and Faculty of Pharmacy, Ton Duc Thang University, Ho Chi Minh City 72915, Vietnam;* orcid.org/0000-0003-1034-1768

Nguyen Thi Mai − *Institute of Materials Science, Vietnam Academy of Science and Technology, Hanoi 11307, Vietnam*

Complete contact information is available at: https://pubs.acs.org/10.1021/acsomega.4c01557

Notes

The authors declare no competing financial interest.

■ ACKNOWLEDGMENTS

The authors thank the financial support of the Vietnam Academy of Science and Technology under the grant no. TDHYD0.04/22-24.

■ REFERENCES

(1) Batool, S.; Nandan, S. P.; Myakala, S. N.; Rajagopal, A.; Schubert, J. S.; Ayala, P.; Naghdi, S.; Saito, H.; Bernardi, J.; Streb, C.; Cherevan, A.; Eder, D. Surface anchoring and active sites of $[Mo_3S_{13}]^{2-}$ clusters as co-catalysts for photocatalytic hydrogen evolution. *ACS Catal.* **2022**, *12*, 6641−6650.

(2) Wu, H.; Huang, Q.; Shi, Y.; Chang, J.; Lu, S. Electrocatalytic water splitting: Mechanism and electrocatalyst design. *Nano Res.* **2023**, *16*, 9142−9157.

(3) Hu, C.; Zhang, L.; Gong, J. Recent progress made in the mechanism comprehension and design of electrocatalysts for alkaline water splitting. *Energy Environ. Sci.* **2019**, *12*, 2620−2645.

(4) Sarwar, S.; Ali, A.; Wang, Y.; Ahasan, M. R.; Wang, R.; Adamczyk, A. J.; Zhang, X. Enhancement of hydrogen evolution reaction activity using metal−rich molybdenum sulfotelluride with graphene support: A combined experimental and computational study. *Nano Energy* **2021**, *90*, 106599.

(5) Yin, H.; Zhao, S.; Zhao, K.; Muqsit, A.; Tang, H.; Chang, L.; Zhao, H.; Gao, Y.; Tang, Z. Ultrathin platinum nanowires grown on single-layered nickel hydroxide with high hydrogen evolution activity. *Nat. Commun.* **2015**, *6*, 6430.

(6) Ma, W.; Zhang, X.; Li, W.; Jiao, M.; Zhang, L.; Ma, R.; Zhou, Z. Advanced Pt-based electrocatalysts for the hydrogen evolution reaction in alkaline medium. *Nanoscale* **2023**, *15*, 11759−11776.

(7) Benck, J. D.; Hellstern, T. R.; Kibsgaard, J.; Chakthranont, P.; Jaramillo, T. Catalyzing the hydrogen evolution reaction (HER) with molybdenum sulfide nanomaterials. *ACS Catal.* **2014**, *4*, 3957−3971.

(8) Medina, M.; Corradini, P. G.; de Brito, J. F.; Sousa Santos, H. L.; Mascaro, L. The substrate morphology effect for sulfur-rich amorphous molybdenum sulfide for electrochemical hydrogen evolution reaction. *J. Electrochem. Soc.* **2022**, *169*, 026519.

(9) Bui, H. T.; Lam, N. D.; Linh, D. C.; Mai, N. T.; Chang, H.; Han, S.-H.; Oanh, V. T. K.; Pham, A. T.; Patil, S. A.; Tung, N. T.; Shrestha, N. K. Escalating Catalytic Activity for Hydrogen Evolution Reaction on $MoSe_2$@Graphene Functionalization. *Nanomaterials* **2023**, *13*, 2139.

(10) Grutza, M.-L.; Rajagopal, A.; Streb, C.; Kurz, P. Hydrogen evolution catalysis by molybdenum sulfides (MoS_x): Are thiomolybdate clusters like $[Mo_3S_{13}]^{2-}$ suitable active site models? *Sustainable Energy Fuels* **2018**, *2*, 1893−1904.

(11) Hellstern, T. R.; Kibsgaard, J.; Tsai, C.; Palm, D. W.; King, L. A.; Abild-Pedersen, F.; Jaramillo, T. F. Investigating catalyst-supporting interactions to improve the hydrogen evolution reaction activity of Thimolybdate $[Mo_3S_{13}]^{2-}$ nanoclusters. *ACS Catal.* **2017**, *7*, 7126−7130.

(12) Kibsgaard, J.; Jaramillo, T. F.; Besenbacher, F. Building an appropriate active-site motif into a hydrogen-evolution catalyst with thiomolybdate $[Mo_3S_{13}]^{2-}$ clusters. *Nat. Chem.* **2014**, *6*, 248−253.

(13) Nguyen, C. T.; Duong, T. M.; Nguyen, M.; Nguyen, Q. T.; Nguyen, A. D.; Dieu Thuy, U. T.; Truong, Q. D.; Nguyen, T. T.; Nguyen, Q. L.; Tran, P. D. Structure and electrochemical property of amorphous molybdenum selenide H_2-evolving catalysts prepared by a solvothermal synthesis. *Int. J. Hydrogen Energy* **2019**, *44*, 13273−13283.

(14) Humphrey, J.; Kronberg, R.; Cai, R.; Laasonen, K.; Palmer, R.; Wain, A. Active site manipulation in MoS_2 cluster electrocatalysts by transition metal doping. *Nanoscale* **2020**, *12*, 4459−4472.

(15) Martinez, L. M.; Delgado, J.; Saiz, C.; Cosio, A.; Wu, Y.; Villagran, D.; Gandha, K.; Karthik, C.; Nlebedim, I.; Singamaneni, S. Magnetic and electrocatalytic properties of transition metal doped MoS_2 nanocrystals. *J. Appl. Phys.* **2018**, *124*, 153903.

(16) Sharma, S.; Ansari, A. Metal and metal oxide sub nanocluster: Emerging aspirant for catalytic application. *Results Chem.* **2023**, *5*, 100982.
(17) Fernández, E.; Boronat, M. Sub nanometer clusters in catalysis. *J. Phys.: Condens. Matter* **2019**, *31*, 013002.
(18) Gong, F.-Q.; Guo, Y.-X.; Fan, Q.-Y.; Cheng, J. Dynamic catalysis of sub-nanometer metal clusters in oxygen dissociation. *Next Nanotechnol.* **2023**, *1*, 100002.
(19) Kagdada, H. L.; Dabhi, S. D.; Jha, P. K. Density functional study of adsorption and desorption dynamics of hydrogen in zirconium doped aluminium clusters. *Int. J. Hydrogen Energy* **2018**, *43*, 21724−21731.
(20) Ma, S.; Fei, S.; Huang, L.; Forrey, R.; Cheng, H. Tuning the catalytic activity of Pd_xNi_y (x+y = 6) bimetallic clusters for hydrogen dissociative chemisorption and desorption. *ACS Omega* **2019**, *4*, 12498−12504.
(21) Lan, N.; Mai, N.; La, D.; Tam, N.; Ngo, S.; Cuong, N.; Dang, N.; Phung, T.; Tung, N. DFT investigation of Au_9Cr^{2+} nanoclusters (M = Sc-Ni): The magnetic superatomic behavior of Au_9Cr^{2+}. *Chem. Phys. Lett.* **2022**, *793*, 139451.
(22) Jia, M.; Vanbuel, J.; Ferrari, P.; Schollkopf, W.; Fielicke, A.; Nguyen, M. T.; Janssens, E. Hydrogen adsorption and dissociation on Al_nRh^{2+} (n = 1 to 9) clusters: Steric and coordination effects. *J. Phys. Chem. C* **2020**, *124*, 7624−7633.
(23) Jia, M.; Vanbuel, J.; Ferrari, P.; Fernandez, E.; Gewinner, S.; Schollkopf, W.; Nguyen, M. T.; Fielicke, A.; Janssens, E. Size dependent H_2 adsorption on Al_nRh^+ (n = 1−12) clusters. *J. Phys. Chem. C* **2018**, *122*, 18247−18255.
(24) Boruah, B.; Kalita, B. Role of 3d transition metal doping in determining the electronic structure and properties of small magnesium clusters: a DFT-based comparison of neutral and cationic states. *J. Nanopart. Res.* **2020**, *22*, 370.
(25) German, E.; Gebauer, R. Improvement of hydrogen vacancy diffusion kinetics in MaH_2 by niobium − and zirconium-doping for hydrogen storage applications. *J. Phys. Chem. C* **2016**, *120*, 4806−4812.
(26) Frisch, M. J. *Gaussian 09*, Revision A02; Gaussian, Inc.: Wallingford CT, 2009.
(27) Tran, P. D.; Tran, T.; Orio, M.; Torelli, S.; Truong, Q. D.; Nayuki, K.; Sasaki, Y.; Chiam, S. Y.; Yi, R.; Honma, I.; Barber, J.; Artero, V. Coordination polymer structure and revisited hydrogen evolution catalytic mechanism for amorphous molybdenum sulfide. *Nat. Mater.* **2016**, *15*, 640−646.
(28) Jiao, H.; Li, Y. W.; Delmon, B.; Halet, J. F. The structure and possible catalytic sites of Mo_3S_9 as a model of amorphous molybdenum Trisulfide: a computational study. *J. Am. Chem. Soc.* **2001**, *123*, 7334−7339.
(29) Tai, T. B.; Nguyen, M. T. A Stochastic Search for the Structures of Small Germanium Clusters and Their Anions: Enhanced Stability by Spherical Aromaticity of the Ge_{10} and Ge_{12} Systems. *J. Chem. Theory Comput.* **2011**, *7*, 1119.
(30) Govind, N.; Petersen, M.; Fitzgerald, G.; King-Smith, D.; Andzelm, J. A generalized synchronous transit method for transition state location. *Comput. Mater. Sci.* **2003**, *28*, 250−258.
(31) Lan, N.; Mai, N.; Cuong, N.; Van, P.; La, D.; Tam, N.; Ngo, S.; Tung, N. Density functional study of size-dependent hydrogen adsorption on Ag_nCr (n = 1 − 12) clusters. *ACS Omega* **2022**, *7*, 37379−37387.
(32) Ortega, G.; Germán, E.; López, M. J.; Alonso, J. A. Catalytic activity of Co-Ag nanoalloys to dissociate molecular hydrogen. New insights on the chemical environment. *Int. J. Hydrogen Energy* **2022**, *47*, 19038−19050.
(33) Kleis, J.; Greeley, J.; Romero, N.; Morozov, V.; Falsig, H.; Larsen, A. H.; Lu, J. M.; Mortensen, J. J.; Dułak, M.; Thygesen, K. S.; Nørskov, J. K.; et al. Finite size effects in chemical bonding: From small clusters to solids. *Catal. Lett.* **2011**, *141*, 1067−1071.
(34) Guo, L. First-principles study of molecular hydrogen adsorption and dissociation on Al_nCr (*n* = 1 - 13) clusters. *J. Phys. Chem. A* **2013**, *117*, 3458−3466.
(35) Lan, N. T.; Mai, N. T.; La, D. D.; Ngo, S. T.; Tam, N. M.; Dang, N. V.; Tung, N. T. Exploring Hydrogen Adsorption on Nanocluster Systems: Insights from DFT Calculations of Au_9M^{2+} (M = Sc - Ni). *Chem. Phys. Lett.* **2023**, *831*, 140838.
(36) Sun, M.; Nelson, A.; Adjaye, J. Adsorption and dissociation of H_2 and H_2S on MoS_2 and NiMo catalysts. *Catal. Today* **2005**, *105*, 36−43.
(37) Afanasiev, P.; Jobic, H. On hydrogen adsorption by nanodispersed MoS_2-based catalysts. *J. Catal.* **2021**, *403*, 111−120.
(38) Baloglou, A.; Plattner, M.; Oncak, M.; Grutza, M.-L.; Kurz, P.; Beyer, M. K. $[Mo_3S_{13}]^{2-}$ as a model system for hydrogen evolution catalysis by MoS_x: Probing protonation sites in the gas phase by infrared multiple photon dissociation spectroscopy. *Angew. Chem., Int. Ed.* **2021**, *60*, 5074−5077.
(39) Chen, Y.; Deng, J.; Yao, W.; Gurti, J. I.; Li, W.; Wang, W.; Yao, J.; Ding, X. Non-stoichiometric molybdenum sulfide clusters and their reactions with the hydrogen molecule. *Phys. Chem. Chem. Phys.* **2021**, *23*, 347−355.
(40) Baloglou, A.; Ončák, M.; Grutza, M.-L.; van der Linde, C.; Kurz, P.; Beyer, M. K. Structural Properties of Gas Phase Molybdenum Sulfide Clusters $[Mo_3S_{13}]^{2-}$, $[HMo_3S_{13}]^-$ and $[H_3Mo_3S_{13}]^+$ as Model Systems of a Promising Hydrogen Evolution Catalyst. *J. Phys. Chem. C* **2019**, *123*, 8177−8186.
(41) Bhatia, S. K.; Myers, A. L. Optimum Conditions for Adsorptive Storage. *Langmuir* **2006**, *22*, 1688−1700.
(42) López-Corral, I.; Germán, E.; Juan, A.; Volpe, M.; Brizuela, G. DFT study of hydrogen adsorption on palladium decorated graphene. *J. Phys. Chem. C* **2011**, *115*, 4315−4323.

https://doi.org/10.1021/acsomega.4c01557
ACS Omega 2024, 9, 20467−20476